

# Adsorption of N<sub>2</sub>O on Cu(100): a combined scanning tunneling microscopy and density functional theory study

K. J. Franke,<sup>\*a</sup> I. Fernández-Torrente,<sup>a</sup> J. I. Pascual<sup>a</sup> and N. Lorente<sup>bc</sup>

Received 1st November 2007, Accepted 19th December 2007

First published as an Advance Article on the web 21st January 2008

DOI: 10.1039/b716952c

The adsorption of N<sub>2</sub>O on Cu(100) has been studied by using scanning tunneling microscopy (STM). In the first molecular layer N<sub>2</sub>O forms a densely packed  $c(3 \times 2)$  structure, in which the molecules occupy two different adsorption sites. The bonding strength of this layer is found to be very weak as revealed by a low desorption temperature and the formation of misalignments and defects. Density functional theory (DFT) finds a stable  $c(3 \times 2)$  structure in which the molecules are considerably bent due to charge transfer. In model calculations for a  $2 \times 2$  hollow phase we show that in order to reach the chemisorbed, bent configuration, the molecules have to pass an activation barrier. In the experimentally accessible range, this is apparently not possible and the molecules remain in a stable physisorbed state.

## 1. Introduction

Molecular binding on solid surfaces is of great interest for the creation of new materials ranging from molecular adlayers with defined patterns to hierarchically grown structures. These materials will have certain characteristics depending on the electronic and geometrical properties of the basic building blocks: the adsorbed molecules. Recently, a lot of effort has been devoted to the study of complex organic molecular arrays<sup>1</sup> showing the promising possibilities of these studies. Yet, not even the simplest molecules are fully understood when they are assembled in contact with a solid surface. An important example is given by the studies of water adlayers that are rapidly advancing in our understanding of the complex intermolecular and molecule–solid interactions.<sup>2</sup> In this framework, the study of triatomic molecules such as water, carbon dioxide and nitrous oxide is of paramount importance. This is not only due to the different types of interactions involved which can unveil complex growth mechanisms, but also because of their predominant role in atmospheric and environmental chemistry. Hence, nitrous oxide (N<sub>2</sub>O) is an extraordinary molecule because of its triatomic asymmetrical shape (the oxygen atom is at one of the molecular ends, see for example ref. 3 and 4) and because it is a dangerous by-product of many industrial processes.<sup>5</sup>

There has been a lot of interest in the catalytic reactions leading to decomposition of N<sub>2</sub>O. Transition metal filaments were soon realized to efficiently dissociate the molecule. This has led to considerable studies of transition metal surfaces in their interaction with N<sub>2</sub>O. An excellent review is the article by Zeigarnik.<sup>6</sup>

In contrast to the filament case, results on dense crystalline surfaces of Cu (notably Cu(100) and Cu(111)) seem to remain under some controversy. Spitzer *et al.*, using ultraviolet photoemission spectroscopy (UPS) complemented with other surface techniques between 90 and 300 K,<sup>7</sup> claim that these surfaces are essentially inert to N<sub>2</sub>O in this temperature range (they find neither dissociation nor adsorption). On the other hand, Johnson *et al.*<sup>8</sup> found that nitrous oxide, which was catalytically formed from NO at 85 K, remains stable on the Cu(100) surface up to 110 K.

At even lower temperatures, near-edge X-ray adsorption fine structure (NEXAFS) experiments<sup>9</sup> have detected molecularly adsorbed N<sub>2</sub>O presenting two distinct phases with different molecular conformation depending on the molecular density: in the high coverage regime, the molecules are found to be almost linear with the terminal nitrogen bonding to the surface. At lower coverages the authors find a bent configuration binding to the surface through both the central and the terminal nitrogen atom. These configurations have been confirmed by multiple scattering simulations of NEXAFS and cluster electronic structure calculations.<sup>10</sup> The bent configurations were shown to be stabilized by charge transfer to the molecules.<sup>4</sup> As the molecule bends the degeneracy of the  $3\pi^*$  orbitals is broken and the energy of the in-plane orbital is lowered. Hence, a partially filled LUMO  $3\pi^*$  orbital energetically favors a bent geometry of the molecule and the bending can be associated with a chemisorption process. However, the exact structure of the bent species contrasts drastically with results from density functional theory (DFT) calculations on more reactive surfaces.<sup>11,12</sup> There, a bent conformation is also found but with the molecule binding to the surface through the terminal nitrogen (N<sub>t</sub>) and the oxygen atom.

Aiming to solve this puzzle, we study here the adsorption of N<sub>2</sub>O on Cu(100) using a combination of low temperature scanning tunneling microscopy (STM) and DFT calculations. Contrary to previous work, we can identify the local adsorption structure with STM. At low coverage and temperatures below 100 K, we observe a  $c(3 \times 2)$  structure that evolves into

<sup>a</sup> Institut für Experimentalphysik, Freie Universität Berlin, Arnimallee 14, 14195 Berlin, Germany. E-mail: franke@physik.fu-berlin.de

<sup>b</sup> LCAR (UMR 5589), Université Paul Sabatier, 118 route de Narbonne, 31062 Toulouse, Cédex France

<sup>c</sup> Centro de Investigación en Nanociencia y Nanotecnología, CSIC-ICN, Campus de la UAB, E-08193 Bellaterra, Spain

a hexamer phase at higher coverage. Moreover, STM allows to determine the adsorption state as weakly physisorbed. DFT permits us to characterize the molecular structures found experimentally. Our findings are that: (i)  $\text{N}_2\text{O}$  adsorbs molecularly on two different sites giving rise to the hybrid  $c(3 \times 2)$  structure; (ii) there are two stable adsorption wells, one corresponding to a bent molecule and to chemisorption, the other one corresponding to a linear molecule and to physisorption; (iii) very low-coverage phases are not stable and lead to dissociation of  $\text{N}_2\text{O}$  on  $\text{Cu}(100)$ .

The article is organized as follows: first we present the experimental method and results; next the computational methods and results, followed by an extensive discussion characterizing the found systems. The presentation of the work is finished by a conclusion section.

## 2. Experiment

All experiments have been carried out under ultra-high vacuum conditions, where the  $\text{Cu}(100)$  sample was prepared by cycles of  $\text{Ne}^+$  sputtering, followed by annealing to 800 K. The cleanliness of the  $\text{N}_2\text{O}$  gas was checked by a mass spectrometer prior to deposition on the surface. The gas was then let into the chamber in a partial pressure range in the  $10^{-8}$  mbar while the sample was kept at the corresponding adsorption temperature. All STM imaging was performed at 5 K.

### Experimental results

The deposition of  $\text{N}_2\text{O}$  on  $\text{Cu}(100)$  has been investigated at sample temperatures of 30 K and above 80 K. The maximum temperature to find adsorption on the surface is around 100 K. Below this critical temperature the adsorption does not show any temperature dependence. As an example of the observed structures, Fig. 1 shows a large scale scanning tunneling microscopy image after an exposure of 0.2 L

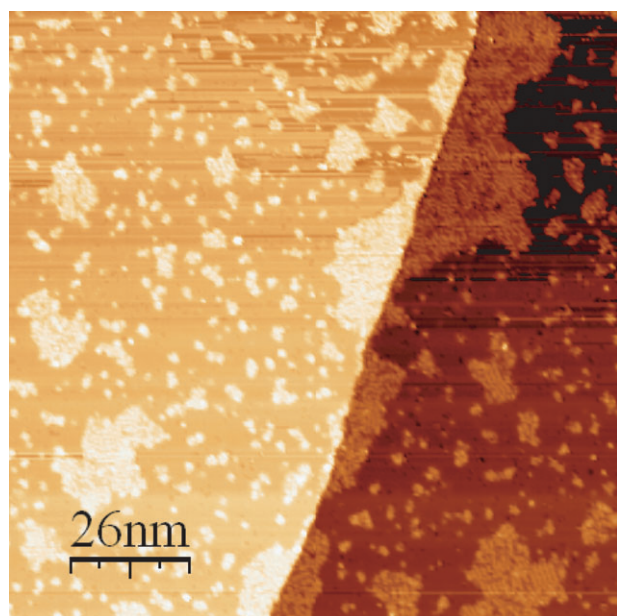


**Fig. 1** STM image ( $I = 0.18$  nA,  $U = 140$  mV) of a large section of the  $\text{Cu}(100)$  surface after exposure of 0.2 L at 100 K.<sup>16</sup>

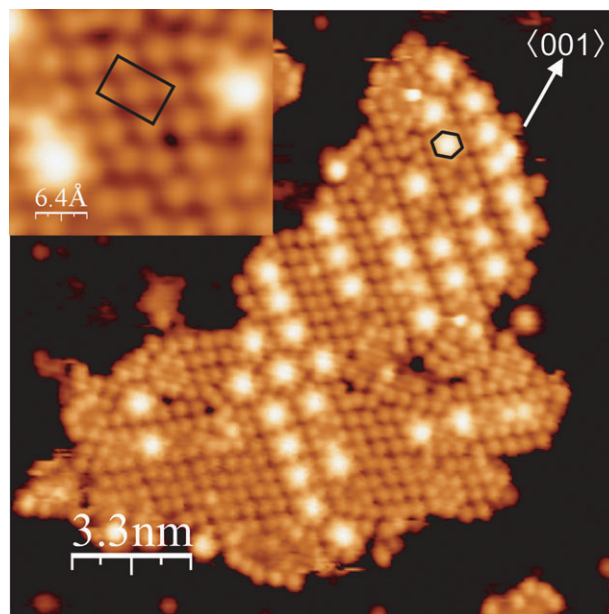


**Fig. 2** STM image ( $I = 0.11$  nA,  $U = 140$  mV) of an  $\text{N}_2\text{O}$  island on  $\text{Cu}(100)$  after an exposure of 0.2 L at 100 K. In this island an ordered  $c(3 \times 2)$  structure is revealed in the first molecular layer. In order to increase the packing density, hexagonal structures are formed with an additional molecule in the center (about  $1/3$  of the molecular adlayer). The inset shows a close-up view of the  $c(3 \times 2)$  structure with the corresponding unit-cell. Each protrusion corresponds to a single  $\text{N}_2\text{O}$  molecule.

at 100 K. The  $\text{N}_2\text{O}$  molecules are imaged as protrusions with an apparent height of  $0.8 \pm 0.1$  Å, which form islands of various sizes. A close-up view of one of the islands is presented in Fig. 2. This island shows a large degree of order, while in smaller islands the molecules seem to have a smaller tendency to form ordered molecular arrays. The ordered structures found within the islands can be classified as follows. The basic structure is a rhombic unit. Based on the corresponding dimensions and the orientation with respect to the substrate a  $c(3 \times 2)$  molecular superstructure can be inferred. While this adsorption structure is commensurate with the substrate, many dislocations can be found within the molecular layer. Additionally, there are also brighter protrusion with an apparent height of  $1.5 \pm 0.1$  Å, which reconstruct the underlying rhombic layer into hexagonal-like shapes (see the hexagon in Fig. 2). These hexamers order themselves following the chain direction of the  $c(3 \times 2)$  layer, but are not fully commensurate with the substrate. We believe that this reorganization is due to an increase in packing density. In order to test this assumption we have deposited a larger amount of  $\text{N}_2\text{O}$  onto the substrate. Indeed, after dosing 1 L at 90 K we obtain an increase in hexamers which replace the  $c(3 \times 2)$  structure (see Fig. 3).

It is remarkable that the intermolecular interactions can easily perturb the molecule surface interaction, thus pointing toward a weakly bound adsorption state. The relatively weak bonding is also revealed by manipulation of adsorbed molecular patches with the STM tip. During the scanning it is possible to break the ordered structures of an island such that the molecules can attach at different adsorption sites. An

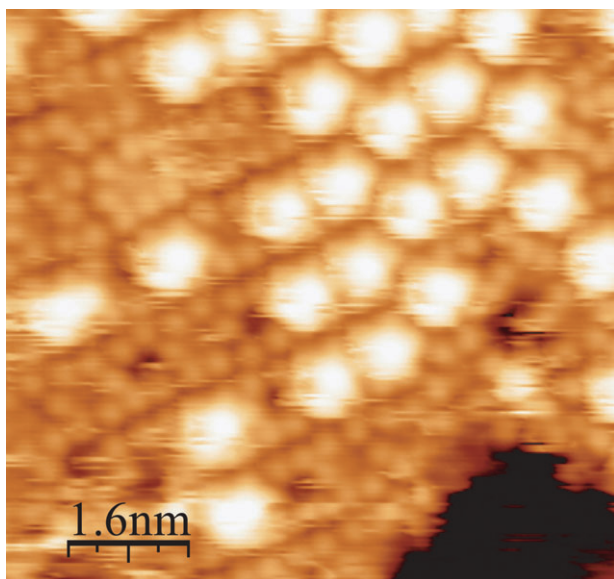


**Fig. 3** After an exposure of 1 L at 90 K a high packing density of  $\text{N}_2\text{O}$  induces the reconstruction of the  $c(3 \times 2)$  structure toward hexamers which yield preferable adsorption sites for second layer molecules ( $I = 0.12$  nA,  $U = 300$  mV). The patches of a  $c(3 \times 2)$  are completely removed. Each protrusion corresponds to a single  $\text{N}_2\text{O}$  molecule.

example is shown in Fig. 4, where a several-nanometre-large part of the island is displaced.

A further indication of the small interaction is given by the low desorption temperature. Annealing this island structure to 125 K leaves only a small amount of clusters on the surface which are preferentially pinned at step edges. Since no oxygen is observed after the annealing, we presume that, under these conditions,  $\text{N}_2\text{O}$  does not undergo dissociative pathways prior to desorption.

We may then conclude that  $\text{N}_2\text{O}$  can adsorb molecularly on Cu(100) at temperatures below or in the order of 100 K. From the loss of commensuration by inclusion of a large number of defects and the creation of hexamers at larger coverage we cannot only deduce a weak adsorption state, but also infer a

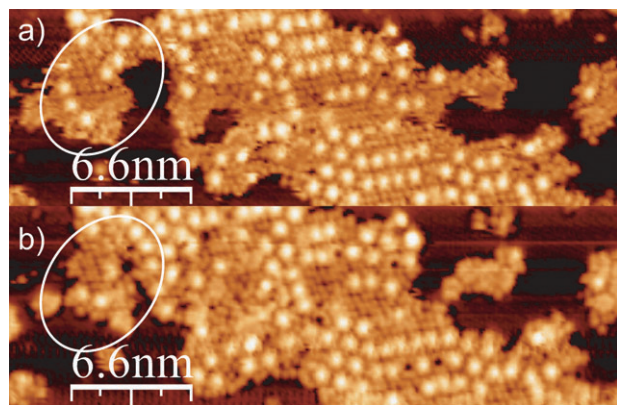


**Fig. 4** Two consecutive STM images of the same  $\text{N}_2\text{O}$  island. The island shape is modified (specially on the left part) during the scanning process ( $I = 0.07$  nA,  $V = 140$  mV) showing that this phase corresponds to a weak interaction with the Cu(100) surface.

physisorbed system. In a chemisorbed phase, on the other hand, a strong site-specificity is expected due to local hybridization with copper electronic states. In order to confirm the formation of such a molecular physisorbed layer, and to gain insight into its detailed structure and properties we analyze the adsorption process using DFT simulations.

### 3. Theory

The planewave ultra-soft pseudopotential code Dacapo<sup>13</sup> has been used to evaluate the total energy, geometrical structure and Kohn–Sham based electronic structure of the molecular adlayers on Cu(100). The approximation for the exchange-and-correlation functional is the GGA of ref. 14 given its accuracy in the description of molecular properties. The structures were relaxed until the forces were smaller than  $0.04$  eV  $\text{\AA}^{-1}$  on the active atoms. The active atoms were the molecular layer (one molecule in the case of the square coverages  $2 \times 2$ ,  $3 \times 3$ ,  $4 \times 4$  and  $6 \times 6$  and 2 molecules for the  $c(3 \times 2)$  coverage) and the 2 topmost layers of the surface slab. This slab contained 5 atomic planes. The calculations were performed for a  $6 \times 6 \times 1$  k-point set for the  $2 \times 2$  structure, after verifying that a  $12 \times 12 \times 1$  k-point set changed the chemisorption energy in less than 10 meV. A consistent k-point set was used for the rest of coverages by keeping the product of the number of surface k-points times the number of surface atoms constant. The total energies are evaluated including a dipole layer in order to correct for the interactions between periodic images of the slab.<sup>13</sup> This correction is mandatory for the kind of system we are dealing with due to the important dipoles developed during the adsorption process.

The chemisorption energy  $E_{\text{chem}}$  is defined as

$$E_{\text{chem}} = E_{\text{N}_2\text{O}/\text{Cu}(100)} - E_{\text{Cu}(100)} - E_{\text{N}_2\text{O}}, \quad (1)$$

where  $E_{\text{N}_2\text{O}/\text{Cu}(100)}$  is the total energy of the relaxed molecule on the surface,  $E_{\text{Cu}(100)}$  is the energy of the relaxed surface and  $E_{\text{N}_2\text{O}}$  is the energy of the relaxed molecule. In a similar way, the energy points of the potential energy surface (PES) correspond to the relaxed system with the convention that the vertical distance between the central N-atom and the surface atom is given by  $Z$ .

The electronic structure is analyzed in terms of the density of states projected on chosen molecular orbitals. This projected density of states (PDOS) is given by the following expression (for an example of another chemisorbed system see ref. 15):

$$\text{PDOS}(E) = \sum_{\lambda} |\langle \text{MO} | \lambda \rangle|^2 \delta(\varepsilon_{\lambda} - E) \quad (2)$$

where  $\lambda$  are the labels of the eigenenergies,  $\varepsilon_{\lambda}$ , and eigenstates,  $|\lambda\rangle$ , of the chemisorbed system and MO is the free-molecule state onto which the density of states is projected. MO is calculated for the free molecule distorted to its chemisorption geometry. The PDOS on molecular orbitals yields information of the molecular character of the chemisorbed system. It is more informative than the PDOS on atomic orbitals used in many works on molecular adsorption because it uses the

molecular orbitals as analyzing building blocks of the system's electronic structure.

The induced density permits to analyze the electronic structure of the full system by decomposing the contributions from the different components. The induced density  $\delta\rho$  is defined analogously to eqn (1):

$$\delta\rho_{\text{chem}} = \rho_{\text{N}_2\text{O}/\text{Cu}(100)} - \rho_{\text{Cu}(100)} - \rho_{\text{N}_2\text{O}}, \quad (3)$$

where  $\rho_{\text{N}_2\text{O}/\text{Cu}(100)}$  is the electron density of the full system,  $\rho_{\text{Cu}(100)}$  of the surface but this time keeping the distortion caused by the molecular adsorption, and  $\rho_{\text{N}_2\text{O}}$  is the density of the molecule in the adsorption configuration. Hence, the induced density gives information of the change of electron density due to the interaction by removing the geometrical effects on the density.

### 3.1 Computational results

**3.1.1 The  $c(3 \times 2)$  structure.** The  $c(3 \times 2)$  molecular lattice found in the experiment is consistent with a unit cell with two molecules, each on a different adsorption site. Two possibilities may occur, which can not be discerned in the experiment: the molecules occupying bridge and hollow sites, or top and bridge sites.

The combination of top and bridge sites does not yield a stable adsorption configuration in our DFT simulations. A  $c(3 \times 2)$  molecular structure on hollow and bridge sites, on the other hand, leads to a stable adsorption phase as shown in Fig. 5. Although the adsorption energy of  $-0.0308$  eV appears small this phase nevertheless represents a chemisorbed state due to the following reasons. Both molecules are found at a typical chemisorption distance from the surface ( $2.23$  Å and  $2.51$  Å for the hollow and bridge site, respectively). Moreover, the molecules do not retain their linear shape from the gas phase but are considerably bent (molecular angle of  $127.3^\circ$  and  $149.3^\circ$  on the hollow and bridge site, respectively). Bending the molecule in the neutral state costs energy ( $2.56$  eV), which only charge transfer can compensate for by populating the LUMO  $3\pi^*$  orbital, whose energy is lowered. Finally this leads to an effective chemisorption energy.

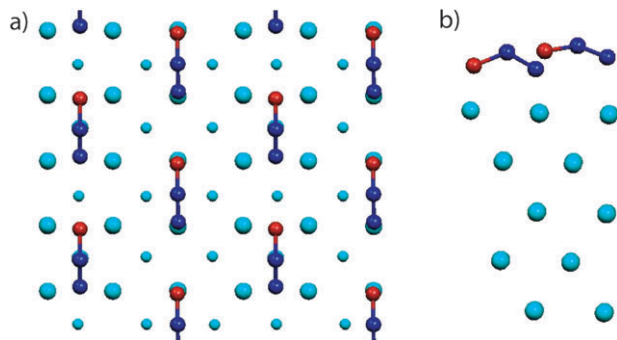


**Fig. 5** Structural model of the  $c(3 \times 2)$  structure as found by DFT simulations with one molecule occupying the hollow and bridge site, respectively, per unit cell. (a) Top view (the first and second lattice plane of Cu(100) are represented by large and small spheres, respectively). (b) Side view: both molecules are bent due to charge transfer and characterize a chemisorbed state.

The existence of a chemisorbed phase in the hollow-bridge structure is an apparent contradiction to the experimental finding of a weakly adsorbed layer. Moreover, we do not find any indication of different adsorption configurations of the  $\text{N}_2\text{O}$  in the bridge or hollow site. In order to investigate the influence of the adsorption sites on the molecular configuration and to understand why an apparently weakly interacting phase is the one found in the experiments, we carried out detailed DFT calculations involving only one type of adsorption site as a model structure, which can be more effectively minimized.

**3.1.2 Comparison of each adsorption site.** A model  $2 \times 2$  structure with one molecule per unit cell has been calculated for each of the possible adsorption sites mentioned above. In all the cases, a stable minimum was obtained, denoting that even in the adsorption state with the highest energy the interaction with the surface is stronger than the van der Waals' one. Table 1 shows the chemisorption energies of the stable molecules on the  $2 \times 2$  hollow (with the molecules oriented along the  $\langle 011 \rangle$  and  $\langle 001 \rangle$ ) direction, top (along  $\langle 011 \rangle$ ) and bridge (along  $\langle 011 \rangle$  and  $\langle 0\bar{1}1 \rangle$ ), as well as the distance of the topmost surface layer to the central nitrogen atom ( $N_c$ ), the molecular angle ( $180^\circ$  correspond to a linear molecule) and the calculated work function change. Fig. 6 shows the geometrical sketches corresponding to the different configurations.

The compilation of results in Table 1 reveals that the molecules on the hollow sites can be found in two significantly different adsorption states. The global minimum of adsorption energy is found when the molecules are located at the shortest distance to the surface. There, they are bent and have a large change in work function, both due to a large change in electronic density. As discussed before, this configuration is characteristic of a considerable charge transfer to the molecule and can hence be associated with a chemisorption state. Additionally, a more weakly adsorbed state with a chemisorption energy of only  $-0.085$  eV can be found further away from the surface at a distance of  $3.2$  Å. In this case the molecule remains close to a linear shape with the terminal nitrogen atom ( $N_t$ ) pointing toward the surface. This state thus corresponds to a physisorbed configuration.

In contrast, the molecules at the top and bridge sites can only be found in a linear conformation. Common to all linear molecules is that the terminal nitrogen atom ( $N_t$  (the closest atom to the surface)) stays at a larger distance than the bent

**Table 1** Adsorption energy,  $E$ , given in eqn (1), for molecules on the  $2 \times 2$  hollow (with the molecular axis aligned along the  $\langle 011 \rangle$  and  $\langle 001 \rangle$  directions), top ( $\langle 011 \rangle$ ), bridge ( $\langle 011 \rangle$  and  $\langle 0\bar{1}1 \rangle$ ), as well as the topmost layer to central atom distance ( $Z$ ), the molecular angle ( $\theta$ ) and the calculated work function change ( $\Delta e\phi$ ). We notice that there are two clear distinct conformations according to the molecular distance to the surface, the molecular angle and the change of work function

	$E/\text{eV}$	$Z/\text{Å}$	$\theta/\text{deg}$	$\Delta e\phi/\text{eV}$
Hollow ( $\langle 001 \rangle$ )	$-0.108$	2.38	141.3	1.425
Hollow ( $\langle 011 \rangle$ )	$-0.113$	2.22	127.7	1.00
Hollow ( $\langle 0\bar{1}1 \rangle$ )	$-0.085$	3.20	177.3	$-0.233$
Top ( $\langle 011 \rangle$ )	$-0.106$	3.49	179.2	$-0.060$
Bridge ( $\langle 011 \rangle$ )	$-0.076$	3.44	178.7	$-0.112$
Bridge ( $\langle 0\bar{1}1 \rangle$ )	$-0.097$	3.42	178.4	$-0.150$

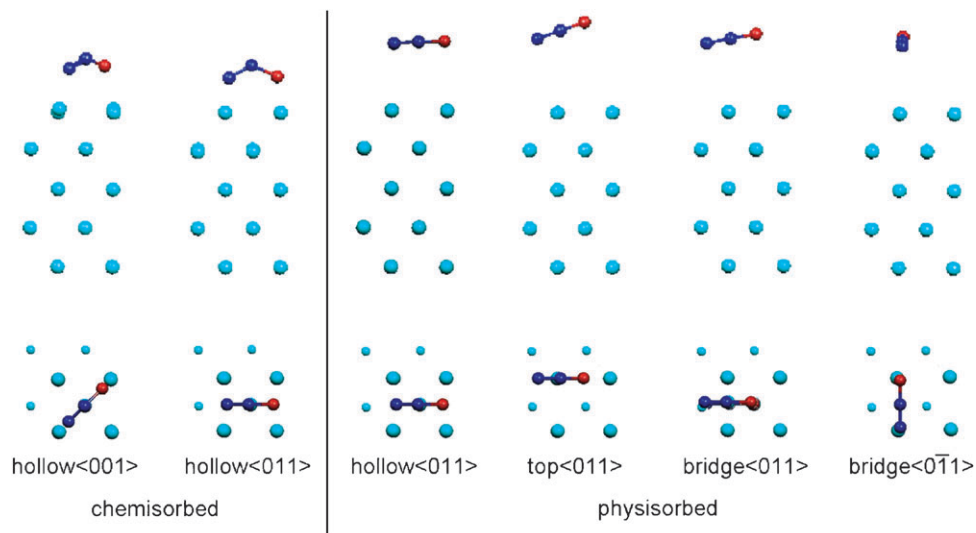


**Fig. 6** Adsorption configurations of Table 1 (top and side views), for molecules on the  $2 \times 2$  hollow (with the molecular axis aligned along the  $\langle 011 \rangle$  and  $\langle 001 \rangle$  directions), top ( $\langle 011 \rangle$ ), bridge ( $\langle 011 \rangle$  and  $\langle 0\bar{1}1 \rangle$ ). In the top view, the first and second lattice plane of Cu(100) are represented by large and small spheres, respectively.

species on the hollow sites (larger than  $3 \text{ \AA}$ ). At first glance, the fact that the molecules are found at a large distance to the surface with a small chemisorption energy renders these calculations questionable. Moreover, the minima found for the adsorption states are rather shallow, *i.e.* the adsorption energy does not strongly depend on the distance to the surface. However, the fact, that we do find a stable minimum and a consistent behaviour throughout the different configurations studied here, shows that there are electrostatic interactions present in the system. Possibly, these arise from the lone pair electrons of the terminal nitrogen atom. Hence, although DFT fails to account for van der Waals forces, the presence of these interactions nevertheless yields a true adsorption state also for the linear  $\text{N}_2\text{O}$  molecule.

The charging of the LUMO for the chemisorbed species (at hollow sites) is revealed when plotting the projected density of states on molecular orbitals, PDOS, eqn (2). The PDOS on the LUMO shows the density of those states of the combined system which possess some LUMO character. In case of a free molecule, the HOMO and LUMO are unperturbed and hence represented as sharp lines on the PDOS. For the chemisorbed molecules we see that basically half of the states which exhibit LUMO character are below the Fermi level (Fig. 7). This is a clear signature of charge transfer from the substrate into the molecule. However, back donation is small. Indeed, the PDOS onto the HOMO corresponds to states that are all below the Fermi level, implying that the molecule does not transfer electrons into the substrate. The interaction of the HOMO with the substrate is not negligible, giving rise to a PDOS that is considerably widened. The LUMO + 1 shows little interaction with the substrate since it maintains an overall lorentzian shape.

In order to confirm charge donation into the LUMO, Fig. 8 shows the induced electron density, eqn (3). In agreement with the density plots of ref. 12, we find that the extra density is due to the filling of the LUMO. This confirms the information obtained from the PDOS analysis.

The induced density, Fig. 8, hints at the creation of a large dipole on the surface as a consequence of this chemisorbed phase. The origin of the dipole can be traced back to the bending of the molecule because of the increasing polarizability (the free molecule dipole is very small) and because of the partial occupation of the LUMO. Associated to this dipole perpendicular to the surface is an increase of the work function (as large as 1 eV).

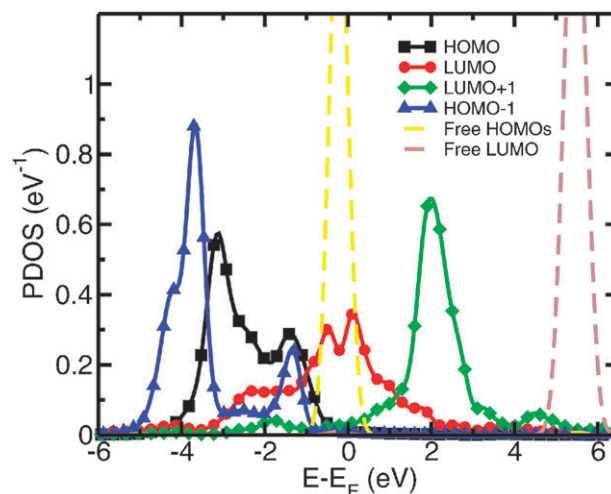


**Fig. 7** Projected density of states on selected molecular orbitals following eqn (2). For the free  $\text{N}_2\text{O}$  molecule the HOMO is twofold degenerate. The HOMO and LUMO (dashed line) are sharp (computational broadening of 0.3 eV). The solid lines represent the PDOS on the HOMO-1, HOMO, LUMO and LUMO + 1 for molecules on the  $2 \times 2$  hollow  $\langle 011 \rangle$ . We notice small distortions from a Lorentzian shape for the LUMO + 1, indicating the small role of this orbital in the chemisorption process. However, the degeneracy of the HOMO is lifted and both the HOMO and the LUMO are considerably widened and distorted by the presence of the surface. Most interesting, the LUMO is largely occupied now, implying strong charge transfer from the substrate.

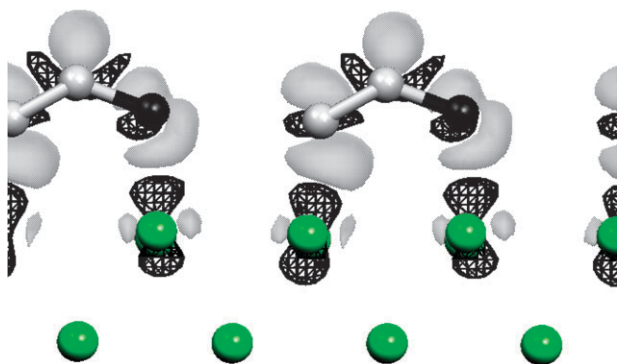


**Fig. 8** Induced charge density on a  $2 \times 2$   $\text{N}_2\text{O}$  molecular adlayer in the hollow  $\langle 011 \rangle$  configuration. The excess charge adopts the profile of the distorted  $3\pi^*$  orbital (LUMO), in the present symmetry corresponding to the  $10a$  orbital.<sup>4</sup> This graph complements the findings of Fig. 5.

The physisorbed species show a contrasting behaviour. Here, no charge transfer into the molecule is observed leading to a very small change in work function with opposite sign. Hence, a very small dipole is pointing in the opposite direction as in the chemisorbed phase.

In conclusion, the DFT simulations find two significantly different adsorption states on a model  $2 \times 2$  structure: a chemisorbed phase characterized by a large amount of charge transfer on the hollow site and a physisorbed configuration on all three adsorption sites, *i.e.* hollow, bridge and top sites. In the experiment on the other hand, we do not have evidence of any chemisorbed species, as revealed by a weak adsorption and weak lateral ordering. Therefore, the question remains, why we do not reach the chemisorbed state under the experimentally accessible conditions. This discrepancy is characteristic of systems with an activation barrier for chemisorption.

**3.1.3 Activation barrier for chemisorption.** In order to fully account for the adsorption pathway which would lead to the chemisorbed state, a multidimensional simulation including various possible adsorption sites, molecular orientations and intermolecular interactions would be required. These calculations are very demanding specially, since the starting point is a physisorbed state with a rather flat potential energy surface. We therefore choose a smaller model structure as a reasonable approach to explore the origin of the activation barrier. Recalling that the  $c(3 \times 2)$  structure consists of molecules on hollow  $\langle 011 \rangle$  and bridge  $\langle 011 \rangle$  sites, the best option is to take one of these in their  $2 \times 2$  configuration. Since the  $2 \times 2$  bridge  $\langle 011 \rangle$  does not exhibit a chemisorption minimum, the corresponding simulation is not suitable and we restrict ourselves to evaluating the adsorption energy of the hollow  $2 \times 2$  structure as a function of the distance to the surface.

Fig. 9 shows the potential energy surface along the normal to the surface for an approaching  $2 \times 2$   $\text{N}_2\text{O}$  molecular adlayer on the hollow  $\langle 011 \rangle$  sites. All degrees of freedom are allowed to minimize the total energy except for the coordinates of the central nitrogen atom  $\text{N}_c$ . Hence, we have plotted the chemisorption energy *versus* the  $\text{N}_c$  vertical distance to the topmost surface layer. The zero of energy is the free molecule

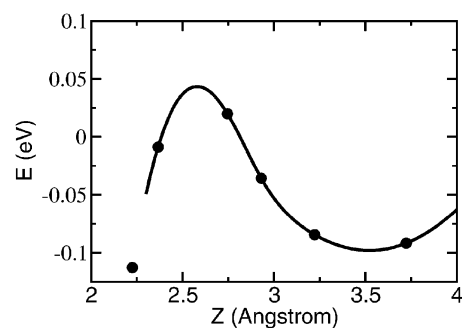


**Fig. 9** Potential energy surface along the normal to the surface for an approaching  $2 \times 2$   $\text{N}_2\text{O}$  molecular adlayer. The energy,  $E$ , is defined according to eqn (1). The distance,  $Z$ , is given by  $\text{N}_c$ -topmost layer distance. The calculated points are represented by dots. The line is a cubic spline intended as a guide-to-the-eye.

plus the totally relaxed clean surface energies, according to the energy definition of eqn (1).

In this plot of the potential energy surface we find an additional local minimum at  $\sim 3.5$  Å. We found 3.2 Å by using a conjugate gradient relaxation with a convergence criterium of  $0.04 \frac{\text{eV}}{\text{\AA}}$  which may lead to a large error bar in the determination of the absolute minimum. Hence, the actual stable distance may be closer to 3.5 Å. Here, in consistency with the larger distance to the surface, the molecules adopt a linear configuration. Therefore, we assign this minimum to a stable weakly adsorbed state. The corresponding adsorption energies, eqn (1), are in the range of 0.1 eV. Due to the absence of dispersive forces in these calculations, this value is probably a lower boundary to the chemisorption energy. Indeed, the observed adsorption temperatures of  $\sim 100$  K indicate adsorption energies rather in the order of 0.3 eV as a first-order desorption dynamics estimate yields. As mentioned above, we attribute the adsorption to an interaction of electrostatic origin mediated by the lone pair electrons of the terminal nitrogen.

These results indicate that there are two stable adsorption states on the hollow site of Cu(100). The barrier between the physisorbed and chemisorbed wells is roughly 150 meV. This defines a finite activation barrier for chemisorption ( $\sim 50$  meV, Fig. 9). Fig. 9 shows a very sharp decrease of the barrier near the chemisorption minimum. This sharp decrease is due to the rapid filling of the LUMO as the molecule bends and approaches the surface. The barrier can be interpreted as arising from the bending of the molecule as a response to the increase in charge back-donation from the surface. This general concept can be applied to all bent molecules in the  $c(3 \times 2)$  structure, even though the absolute value of the barrier might differ. The existence of this activation barrier may explain why in our experiments the chemisorbed species are not observed.

### 3.2 Dissociative chemisorption

The calculations have also been pursued for smaller coverages at the same degree of accuracy. The final evolution of the molecular system on Cu(100) was dissociation for the unit cells  $3 \times 3$ ,  $4 \times 4$  and  $6 \times 6$ . At smaller coverages, the molecule-substrate interaction becomes increasingly important, leading to a larger charge transfer into the LUMO. The population of

the LUMO favors a stronger bending of the molecule and eventually the dissociation of the O atoms which are strongly bound to the surface. The formed N<sub>2</sub> molecules do not chemisorb on Cu(100).

#### 4. Discussion

Experimentally, N<sub>2</sub>O islands form a network of  $c(3 \times 2)$  molecules following the underlying Cu(100) substrate. The corresponding STM images show a periodic arrangement of similar protrusions and a tendency to accumulate defects in the islands. The layer is weakly bound to the substrate and shows a characteristics of a physisorbed phase.

From the model calculations using a  $2 \times 2$  structure we infer that two adsorption states can be found in this system, a chemisorbed and a physisorbed one. The former exists only at the hollow sites. The latter can be found at each of the three sites explored, top, bridge and hollow. The chemisorption phase is associated with a large charge transfer, and with an important induced dipole with an increase of work function in the order of 1 eV.

In order to understand why experimentally we can not find any chemisorption state, we have performed DFT calculations with a  $2 \times 2$  coverage. These show that the molecule is first attracted into a potential well that lies at about 3 Å from the surface. To reach the well closer to the surface, the molecule needs to surmount a chemisorption barrier. Hence, the likelihood that the molecule ends up in the inner well is rather small. The chemisorbed phases are difficult to attain because of the small window of temperatures and molecular partial pressure at which they might be formed.

We then deduce that the  $c(3 \times 2)$  layer is solely formed by physisorbed molecules, hence having a linear structure with the terminal nitrogen atom pointing towards the surface. We expect that the molecules lie more than 3 Å away from the topmost surface layer and that they exhibit only a small charge transfer. The interactions are very weak and therefore, the layer desorbs soon above the dosing temperatures.

This interpretation of weakly bound linear molecules agrees with the findings by Ceballos *et al.*<sup>9</sup> for their large coverage limit. They observe linear molecules when they approach the monolayer coverage. This interpretation has been confirmed by calculations of the NEXAFS data.<sup>10</sup> The  $c(3 \times 2)$  structure is indeed the largest N<sub>2</sub>O coverage that is possible on this surface. Experimentally, we have found that larger coverages lead to a reconstruction of the first molecular layer by strong intermolecular interactions. From the theoretical simulations we can infer that larger coverages within the same layer underlie strong intermolecular repulsions and are therefore not stable.

In the same report (ref. 9) the authors also investigate a coverage of 0.5 monolayers. They conclude that under these conditions, the molecules are adsorbed *via* both N atoms, while the O is bent away from the surface. In our experiments, we find that low coverages lead to the formation of small islands, which do not show any apparent ordered structure. Therefore, we are not able to identify fingerprints of molecular states or orientations. However, this configuration seems inconsistent with our calculations as well as with results by

Kokalj *et al.*<sup>11,12</sup> on different transition metal surfaces. A chemisorption state with charge transfer into the molecule yields a bending such that the O atom always approaches the surface.

#### 5. Conclusions

The combined experimental and theoretical study has permitted us to characterize the adsorption of N<sub>2</sub>O on Cu(100). For deposition temperatures below 100 K, different sizes of N<sub>2</sub>O islands are observed depending on the molecular dosing. The islands can show ordered structures but are prone to defect formation and, in the low coverage limit they show no order. The ordered phase corresponds to  $c(3 \times 2)$  molecular arrangements with respect to the underlying Cu(100) substrate. At larger dosing, the packing density is increased by a reconstruction of the  $c(3 \times 2)$  adlayer into hexagonal structures, which are not fully commensurate with the substrate. At 125 K even molecules pinned to step edges disappear.

Theoretically, only the  $2 \times 2$  and  $c(3 \times 2)$  coverage are stable on Cu(100). The hollow  $2 \times 2$  structure exists in two adsorption states: a weakly bound configuration at  $\sim 3.5$  Å from the surface, where the molecules conserve their linear shape and a chemisorbed state at 2.3 Å from the surface plane, where the molecules are bent due to considerable charge transfer into the molecule. For the chemisorbed phase there is an activation barrier, which prevents the molecules in the experiment from going into the chemisorption state. The same holds true for molecules in the  $c(3 \times 2)$  structure, which explains the experimental findings of a weakly adsorbed N<sub>2</sub>O layer on Cu(100). The chemisorbed phases are probably beyond access at the experimental temperatures and partial pressures due to the activation barrier.

#### Acknowledgements

We thank M. Alemani and C. Roth for the construction of the STM. I.F.-T. acknowledges financial support from the Generalitat de Catalunya. Computational resources at the Freie Universität Computational Center, the Centre Informatique National de l'Enseignement Supérieur and the Centre de Calcul Midi-Pyrénées are gratefully acknowledged. The authors also acknowledge support of DAAD. This joint work has been made possible by the funding of the Franco-German bilateral program PROCOPE.

#### References

- 1 A. Dimitriev, H. Spillmann, N. Lin, J. V. Barth and K. Kern, *Angew. Chem., Int. Ed.*, 2003, **42**, 2670.
- 2 (a) A. Verdager, G. M. Sacha, H. Bluhm and M. Salmeron, *Chem. Rev.*, 2006, **106**, 1478; (b) J. Cerdá, A. Michaelides, M.-L. Bocquet, P. J. Feibelman, T. Mitsui, M. Rose, E. Fomin and M. Salmeron, *Phys. Rev. Lett.*, 2004, **93**, 116101.
- 3 G. Herzberg, *Molecular Spectra and Molecular Structure III. Electronic Spectra and Electronic Structure of Polyatomic Molecules*, D. Van Nostrand Co., Inc., Princeton, N.J., 1966, p. 595.
- 4 S. D. Peyerimhoff and R. J. Buenker, *J. Chem. Phys.*, 1968, **49**, 2473.
- 5 F. Kapteijn, J. Rodriguez-Marisol and J. A. Moulijn, *Appl. Catal., B*, 1996, **9**, 25.
- 6 A. V. Zeigarnik, *Kinet. Catal.*, 2003, **44**, 233.

- 7 A. Spitzer and H. Lüth, *Phys. Rev. B*, 1984, **30**, 3098.  
8 D. W. Johnson, M. H. Matloob and M. W. Roberts, *J. Chem. Soc., Chem. Commun.*, 1978, 40.  
9 G. Ceballos, H. Wende, K. Baberschke and D. Arvanitis, *Surf. Sci.*, 2001, **482–485**, 15.  
10 T.-Q. Wu, J.-C. Tang, S.-L. Shen, S. Cao and H.-Y. Li, *Chin. Phys. Lett.*, 2004, **21**, 1586.  
11 A. Kokalj, I. Kopal and T. Matsushima, *J. Phys. Chem. B*, 2003, **107**, 2741.  
12 A. Kokalj and T. Matsushima, *J. Chem. Phys.*, 2005, **122**, 034708.  
13 <http://dcwww.camd.dtu.dk/campos/Dacapo/download.html>.  
14 J. P. Perdew, J. A. Chevary, S. H. Vosko, K. A. Jackson, M. R. Pederson, D. J. Singh and C. Fiolhais, *Phys. Rev. B*, 1992, **46**, 6671.  
15 N. Lorente, M. F. G. Hedouin, R. E. Palmer and M. Persson, *Phys. Rev. B*, 2003, **78**, 155401.  
16 All images have been displayed using the WSxM software described in I. Horcas, R. Fernandez, J. M. Gomez-Rodriguez, J. Colchero, J. Gomez-Herrero and A. M. Baro, *Rev. Sci. Instrum.*, 2007, **78**, 013705.

# Find a SOLUTION

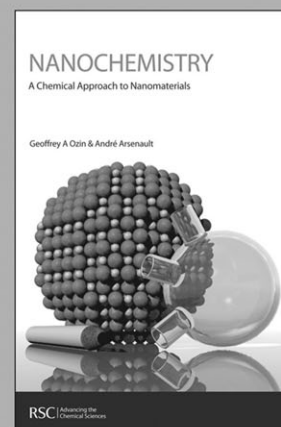
... with books from the RSC

**Choose from exciting textbooks, research level books or reference books in a wide range of subject areas, including:**

- Biological science
- Food and nutrition
- Materials and nanoscience
- Analytical and environmental sciences
- Organic, inorganic and physical chemistry

**Look out for 3 new series coming soon ...**

- RSC Nanoscience & Nanotechnology Series
- Issues in Toxicology
- RSC Biomolecular Sciences Series



RSC Publishing

[www.rsc.org/books](http://www.rsc.org/books)